

ChemComm

Accepted Manuscript



This is an *Accepted Manuscript*, which has been through the Royal Society of Chemistry peer review process and has been accepted for publication.

Accepted Manuscripts are published online shortly after acceptance, before technical editing, formatting and proof reading. Using this free service, authors can make their results available to the community, in citable form, before we publish the edited article. We will replace this *Accepted Manuscript* with the edited and formatted *Advance Article* as soon as it is available.

You can find more information about *Accepted Manuscripts* in the [Information for Authors](#).

Please note that technical editing may introduce minor changes to the text and/or graphics, which may alter content. The journal's standard [Terms & Conditions](#) and the [Ethical guidelines](#) still apply. In no event shall the Royal Society of Chemistry be held responsible for any errors or omissions in this *Accepted Manuscript* or any consequences arising from the use of any information it contains.

Cite this: DOI: 10.1039/c0xx00000x

www.rsc.org/xxxxxx

ARTICLE TYPE

Mesoporous single crystals $\text{Li}_4\text{Ti}_5\text{O}_{12}$ grown on rGO as high-rate anode materials for lithium-ion battery

Weina Chen, Hao Jiang,* Yanjie Hu, Yihui Dai, Chunzhong Li*

Received (in XXX, XXX) Xth XXXXXXXXX 20XX, Accepted Xth XXXXXXXXX 20XX

DOI: 10.1039/b000000x

Mesoporous single crystals $\text{Li}_4\text{Ti}_5\text{O}_{12}$ grown on reduced graphene oxide (MSCs-LTO/rGO) nanohybrids have been synthesized by a simple hydrothermal reaction of TiO_2/rGO and LiOH with subsequent annealing in Ar at 600 °C, which exhibited high specific capacity (171 mAh g^{-1}) with much improved rate capability (132 mAh g^{-1} at 40C) and intriguing cycling stability (85 % capacity retention after 2000 cycles).

Nowadays, lithium-ion batteries (LIBs) offer an attractive option for large-scale applications motivated by clean energy system, such as the electric vehicles (EV) and hybrid electrical vehicles (HEV), due to the advantages of high energy density, high power density and long cycle life.¹ However, as the widely used anode material for commercial LIBs, graphite has a low Li^+ diffusion coefficient, greatly restricting the high-rate performance. In addition, its low operating potential below 0.2 V (*vs.* Li/Li^+) results in the growth of lithium dendrites on the anode surface at the overcharged state, which can cause serious safety issues.² One feasible strategy to address the above drawbacks is to search for an alternative anode material that possesses higher Li-insertion voltage.

Recently, spinel $\text{Li}_4\text{Ti}_5\text{O}_{12}$ (LTO) has attracted plenty of attention as one of the ideal candidates for LIBs anode materials, because a high operating voltage (1.55 V *vs.* Li/Li^+) of LTO makes it safe by avoiding the reduction of electrolytes and Li-metal deposition.^{3,4} In addition, its zero-strain characteristic ensuring excellent reversibility and structural stability, plus fast lithium ion mobility, contribute to the potential for high-rate LIBs applications.³ However, the vital drawback of LTO is the intrinsic insulating property. When discharged at high current densities, the electrode presents serious polarization, leading to poor rate performance. In attempt to overcome this limitation, nanostructured LTO with various morphologies, such as hierarchically porous microsphere,⁵ hollow microsphere assembled by nanosheets,⁶ hollow microsphere,⁷ and so forth, have been developed. In this regard, the nanostructures are beneficial for reducing the diffusion path of ions and electrons and enhancing the intercalation kinetics in view of their high electrode/electrolyte contact area. However, the contact resistance among the nano-sized building blocks cannot be ignored, which may restrict the rate performance of electrode materials to some extent. Very recently, mesoporous single crystals (MSCs) have attracted considerable attention in energy storage fields considering that the unique structure can provide high specific

surface area, long-range electronic connectivity and structure coherence, which can effectively reduce the contact resistance among the building blocks.^{8,9} However, there are only limited reports on the synthesis of MSCs for enhancing LIB performance due to the difficulty in exploring new synthetic protocols. For example, Crossland et al.⁹ fabricated MSCs TiO_2 via a complicated pre-seeding method using silicon as template, delivering substantially higher conductivity and electron mobility than the solid TiO_2 nanocrystals. On the other hand, advanced carbon materials, like CNTs, graphene, have also been introduced into LTO to further enhance the rate capability. In this content, the rational hybridization between MSCs LTO nanoparticles and advanced carbon materials may provide an advanced approach to remarkably improve LIB performance.

Herein, we have successfully realized the synthesis of MSCs LTO nanoparticles supported on reduced graphene oxide (rGO) *via* hydrothermal treatment of TiO_2/rGO and LiOH and the subsequent annealing in Ar at 600 °C. The unique structure, when applied as LIBs anode material, possesses three obvious advantages. (1) The mesoporous feature of LTO nanoparticles, as well as the defects of rGO not only provide more electrochemical active sites, but also promote the strong interaction between electrolyte and active materials. (2) The introduction of rGO can not only greatly improve the conductivity of LTO, but also avoid the aggregation of LTO nanoparticles during the synthesis process. (3) The single crystal nature of LTO helps to decrease the contact resistance and facilitate Li ion diffusion. Based on these advantages, the as-synthesized MSCs-LTO/rGO nanohybrids exhibit high specific capacity with excellent rate capability and long cycle life.

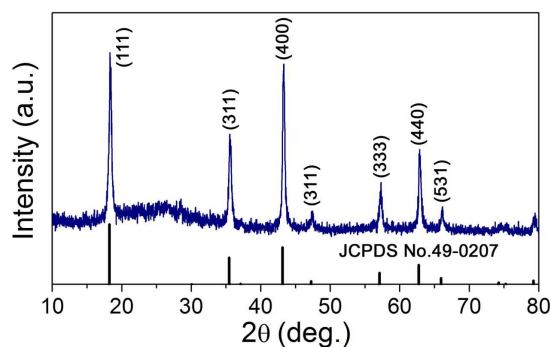


Fig. 1 XRD pattern of the as-prepared MSCs-LTO/rGO nanohybrids.

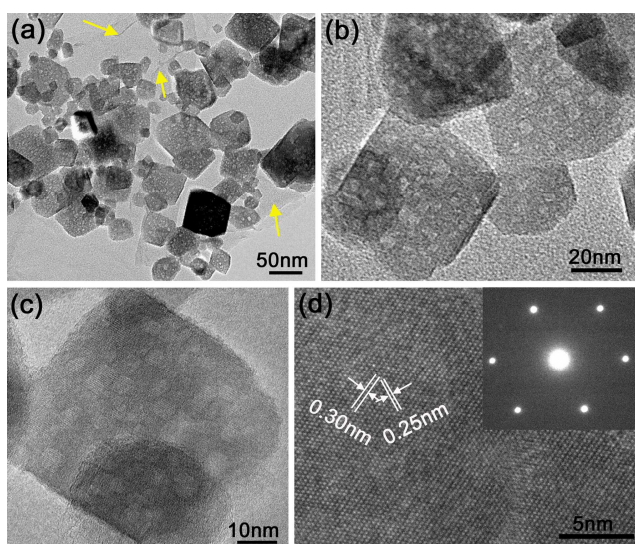


Fig. 2 (a) Low-magnification TEM image of the as-prepared MSCs-LTO/rGO nanohybrids, (b-c) high-magnification and (d) high-resolution TEM images of the MSCs-LTO nanoparticles, inset in (d) showing the corresponding SAED pattern of one nanoparticle.

Fig. 1 shows the XRD pattern of the as-prepared MSCs-LTO/rGO nanohybrids. All the diffraction peaks can be indexed to the spinel $\text{Li}_4\text{Ti}_5\text{O}_{12}$ (JCDPS No. 49-0207). No characteristic peaks of impurities, such as TiO_2 , is observed, indicating the successful growth of LTO on rGO. In addition, the diffraction peaks are considerably sharp, suggesting a highly crystalline nature of the LTO in the sample. The morphology and structure properties of the MSCs-LTO/rGO nanohybrids were examined by transmission electron microscopy (TEM) and high-resolution TEM (HRTEM), as shown in Fig. 2. From the low-magnification TEM image (Fig. 2a), it can be observed that the LTO nanoparticles are well-dispersed on rGO nanosheets (marked by yellow arrows), with an average diameter of ~ 30 -60 nm. Notably, the LTO nanoparticles have a porous feature, which has been further revealed in high-magnification TEM images, as shown in Fig. 2(b-c). A representative LTO nanoparticle is shown in Fig. 2c with a mean pore size of ~ 4 nm. The mesoporous structure offers rich channels for the sufficient interaction between active materials and electrolyte, which can shorten the transfer paths of electrons and Li ions, and thus leading to high capacity and excellent rate capability. The HRTEM image of the LTO is shown in Fig. 2d. The lattice fringes of ~ 0.25 nm and ~ 0.30 nm are ascribed to the (311) and the (220) planes of spinel LTO, respectively. The SAED pattern (inset in Fig. 2d), taken from a random nanoparticle, shows a distinct single crystalline nature. Therefore, MSCs LTO have been successfully realized in the present work. The single crystalline feature will help to increase the conductivity,¹⁵ leading to high electrochemical performance.

To gain further insight into the porous structure and pore size distribution, Brunauer-Emmett-Teller (BET) measurements were performed, as shown in Fig. 3a. The specific surface area of the sample is measured to be about $43.2 \text{ m}^2 \text{ g}^{-1}$. The sample also possesses a bimodal mesopore size distribution with small pores (~ 3.6 nm) from the MSCs LTO and big space (~ 30.0 nm)

possibly from the interlayer space of the LTO/rGO nanosheets.

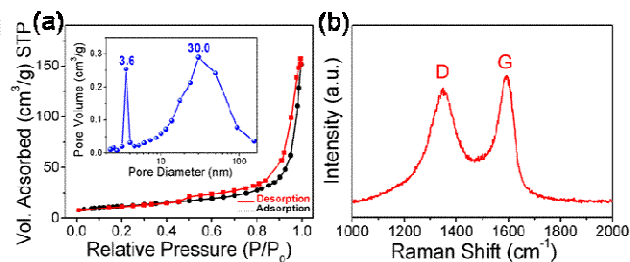


Fig. 3 (a) N_2 adsorption-desorption isotherms and the corresponding pore size distribution (the inset), and (b) Raman spectrum of the as-prepared MSCs-LTO/rGO nanohybrids.

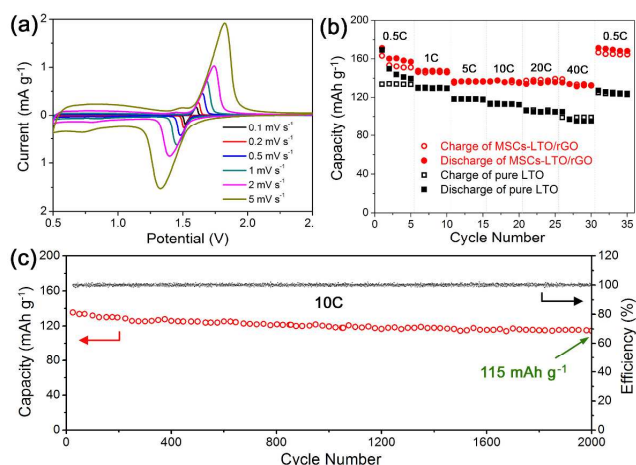


Fig. 4 (a) CV curves of the MSCs-LTO/rGO nanohybrids at different scan rates, (b) the capacity retention of MSCs-LTO/rGO nanohybrids and pure LTO nanoparticles at various current densities, (c) cycling performance of the MSCs-LTO/rGO nanohybrids at 10C for 2000 cycles.

These features are in good agreement with the TEM observations. To investigate the content and the quality of rGO, the sample was further characterized by TG and Raman analysis. The content of rGO is estimated to be $\sim 18\%$ according to the TG curve (Fig. S1). The Raman spectrum displays two main peaks around 1350 cm^{-1} and 1590 cm^{-1} in Fig. 3b, which are assigned to the D-band (the disordered carbon) and the G-band (the ordered graphitic carbon) of rGO, respectively. The relative intensity ratio of D-band and G-band (I_D/I_G), reflects the degree of graphitization. Thus the low value of I_D/I_G (0.92) indicates a highly graphitization degree,¹⁰ which is conducive to the improvement of electrical conductivity.

The electrochemical performance of the MSCs-LTO/rGO nanohybrids was evaluated by assembling the materials into 2016 coin cells. Fig. 4a shows the cyclic voltammograms (CV) curves at scan rates of 0.1 - 5 mV s^{-1} in the voltage range of 0.5 - 2.5 V (vs. Li/Li^+). Each CV curve exhibits a couple of sharp redox peaks centered at 1.3 V and 1.8 V , corresponding to the characteristic peaks of Li^+ insertion/extraction in spinel LTO.¹¹ Moreover, the peaks still retain a stable and sharp shape even at a scan rate as high as 5 mV s^{-1} , indicating the fast Li^+ insertion/extraction kinetics.¹² Besides, to identify the reversibility of the Li^+ insertion/extraction process, the ratio of anodic peak current to cathodic peak current (I_{pa}/I_{pc}) should be equal to unity

theoretically. From the symmetric curves, the value of I_{pa} is closely approaching to that of I_{pc} , showing the high reversible capacity. These results suggest the high rate capability of the as-synthesized MSCs-LTO/rGO nanohybrids.

To evaluate the rate performance, the MSCs-LTO/rGO electrode was charged and discharged at various current rates within a potential window of 1-2.5 V, as shown in Fig. 4b. It can be observed that the first cycle at a low rate of 0.5C obtains a high specific capacity of 171 mAh g⁻¹ with a high Coulombic efficiency (CE) of ~ 95.6% (Fig. S2), which is close to the theoretical capacity (175 mAh g⁻¹) of spinel LTO. Even at a high rate of 40C, the capacity still retains 132 mAh g⁻¹. When the current density returns back to 0.5C after cycling at various rates, a high capacity of 171 mAh g⁻¹ is recovered. To make a contrast, pure LTO was also prepared using a similar method without the addition of GO, which shows an aggregation composed of numerous nanoparticles with diameters of ~ 50-100 nm (Fig. S3). The pure LTO anode materials exhibit a capacity of 169 mAh g⁻¹ at 0.5C with a decreased CE of ~ 79.1% and a poor rate capability (100 mAh g⁻¹ at 40C). And more significantly, the LIB performance of MSCs-LTO/rGO nanohybrids is remarkably improved compared with those of the other reported LTO/rGO nanohybrids.^{4,13} Recently, Shen et al.¹³ developed in situ growth strategy to obtain graphene-supported LTO nanoparticles, delivering an inferior rate capability of 82.7 mAh g⁻¹ at 30C. The intriguing electrochemical performance of our sample can be mainly ascribed to MSCs feature as well as the strong coupling effects between LTO and rGO. In this structure, rGO has dual functions, which can not only accelerate the electron transfer, but also avoid the aggregation of MSCs LTO nanoparticles during the synthesis process. The direct evidence is the SEM image of pure LTO nanoparticles (Fig. S3). Moreover, the defects of rGO from the preparation process can also improve electrochemical performance.¹⁴ The electrochemical impedance spectra of the MSCs-LTO/rGO nanohybrids and the pure LTO nanoparticles are also provided (Fig. S4). The diameter of the semi-circle at high frequencies is greatly reduced in the plot of the MSCs-LTO/rGO nanohybrids, indicating the remarkably decreased charge-transfer resistance at the electrode/electrolyte interface due to the introduction of rGO.^{15,16} A detailed discussion has been provided in ESI. The improved electronic and ionic conductivity favours the electron and Li ions transfer in the electrode, which further confirms our results. The MSCs-LTO/rGO nanohybrids also have excellent cycling stability. Fig. 4c gives the discharge capacity and the corresponding CE as a function of cycle number at 10C. The discharge capacity displays an unobscured decay, and it still delivers a capacity of as high as 115 mAh g⁻¹ even after 2000 cycles (~ 85% capacity retention). In addition, the efficiency also keeps steady at ~ 100 % during the whole cycling process. Such superior cycling stability indicates that if the as-obtained anode material was employed in electric vehicles, it could enable the battery to be rapidly charged without remarkable degradation.

Conclusions

In summary, the MSCs-LTO/rGO nanohybrids were successfully prepared by a simple hydrothermal reaction of TiO₂/rGO and LiOH with subsequent annealing in Ar at 600 °C.

The MSCs LTO nanoparticles possess a diameter of ~ 30-60 nm with a bimodal mesopore structure. The smart MSCs-LTO/rGO nanohybrids, as LIBs anode material, exhibit a high specific capacity of 171 mAh g⁻¹ at 0.5C with excellent rate capability (132 mAh g⁻¹ at 40C). More significantly, the hybrids demonstrate a long-term cycle life for LIBs (85% capacity retention after 2000 cycles). Such excellent electrochemical performances are mainly attributed to the MSCs feature of LTO nanoparticles as well as the strong coupling effects between LTO and rGO. The present work indicates that MSCs nanoparticles combined with advanced carbon materials should be a promising approach to improve the rate capability of electrode materials.

This work was supported by the National Natural Science Foundation of China (21136006, 21236003), the Basic Research Program of Shanghai (13JC1401901), the Program for New Century Excellent Talents in University (NCET-13-0796), and the Program for Professor of Special Appointment (Eastern Scholar) at Shanghai Institutions of Higher Learning.

Notes and references

Key Laboratory for Ultrafine Materials of Ministry of Education, School of Materials Science and Engineering, East China University of Science and Technology, Shanghai 200237, China. Fax: +86-21-64250624; Tel: +86-21-64250949; E-mail: jianghao@ecust.edu.cn (H. Jiang) and czli@ecust.edu.cn (C. Z. Li).

† Electronic Supplementary Information (ESI) available: [Experimental details, TG and EIS analysis and SEM images of pure LTO]. See DOI: 10.1039/b000000x/

- (a) K. Amine, I. Belharouak, Z. Chen, T. Tran, H. Yumoto, N. Ota, S. T. Myung and Y. K. Sun, *Adv. Mater.*, 2010, **22**, 3052-3057; (b) J. Yan, A. Sumboja, E. Khoo and P. S. Lee, *Adv. Mater.*, 2011, **23**, 746; (c) S. Guo and S. Dong, *Chem. Soc. Rev.*, 2011, **40**, 2644-2672.
- (a) L. Shen, X. Zhang, E. Uchaker, C. Yuan and G. Cao, *Adv. Energy Mater.*, 2012, **2**, 691-698; (b) Z. Liu, N. Zhang and K. Sun, *J. Mater. Chem.*, 2012, **22**, 11688.
- L. Shen, E. Uchaker, X. Zhang and G. Cao, *Adv. Mater.*, 2012, **24**, 6502-6506.
- (a) M. S. Song, A. Benayad, Y. M. Choi and K. S. Park, *Chem. Comm.*, 2012, **48**, 516; (b) Y. Shi, L. Wen, F. Li and H. M. Chen, *J. Power Sources*, 2011, **196**, 8610-8617.
- L. Shen, C. Yuan, H. Luo, X. Zhang, K. Xu and Y. Xia, *J. Mater. Chem.*, 2010, **20**, 6998.
- Y. Tang, L. Yang, S. Fang and Z. Qiu, *Electrochim. Acta*, 2009, **54**, 6244-6249.
- L. Yu, H. B. Wu and X. W. D. Lou, *Adv. Mater.*, 2013, **25**, 2296-2300.
- (a) X. W. Lou, D. Deng, J. Y. Lee and L. A. Archer, *J. Mater. Chem.*, 2008, **18**, 4397-4401; (b) J. F. Ye, W. Liu, J. G. Cai, S. A. Chen, X. W. Zhao, H. H. Zhou and L. M. Qi, *J. Am. Chem. Soc.*, 2011, **133**, 933-940.
- E. J. Crossland, N. Noel, V. Sivaram, T. Leijtens, J. A. Alexander Webber and H. J. Snaith, *Nature*, 2013, **495**, 215-219.
- B. Li, C. Han, Y. B. He, C. Yang, H. Du, Q. H. Yang and F. Kang, *Energy Environ. Sci.*, 2012, **5**, 9595.
- Y. Wang, H. Liu, K. Wang, H. Eiji, Y. Wang and H. Zhou, *J. Mater. Chem.*, 2009, **19**, 6789.
- B. Zhang, Y. Liu, Z. Huang, S. Oh, Y. Yu, Y. W. Mai and J. K. Kim, *J. Mater. Chem.*, 2012, **22**, 12133.
- L. Shen, C. Yuan, H. Luo, X. Zhang, S. Yang and X. Lu, *Nanoscale*, 2011, **3**, 572-574.
- (a) F. Banhart, J. Kotakoski and A. V. Krasheninnikov, *ACS Nano*, 2011, **5**, 26-41; (b) D. Li, D. Shi, H. Liu and Z. Guo, *J. Nanopart. Res.*, 2013, **15**, 1674.
- Z. Liu, Z. Cao, B. Deng, Y. Wang, J. Shao, P. Kumar, C. R. Liu, B. Wei and G. J. Cheng, *Nanoscale*, 2014, **6**, 5853-5858.
- L. Sun, J. Wang, K. Jiang and S. Fan, *J. Power Sources*, 2014, **248**, 265-272.

5 TOC

